GEOLOGY OF THE LUNAR CRATER VOLCANIC FIELD, NYE COUNTY, NEVADA

CONTRIBUTIONS TO ASTROGEOLOGY

Prepared on behalf of the National Aeronautics and Space Administration

GEOLOGICAL SURVEY PROFESSIONAL PAPER 599-I

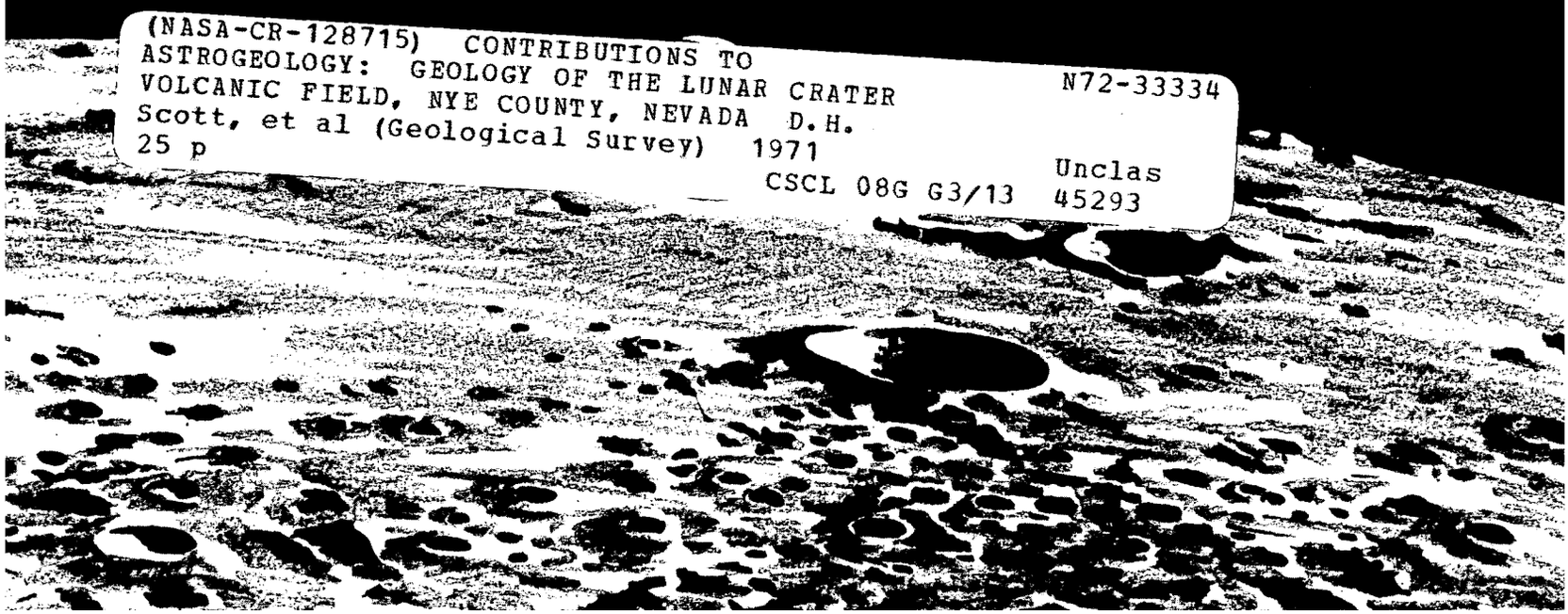

SGT

Geology of the Lunar Crater Volcanic Field, Nye County, Nevada

By DAVID H. SCOTT *and* N. J. TRASK

CONTRIBUTIONS TO ASTROGEOLOGY

GEOLOGICAL SURVEY PROFESSIONAL PAPER 599-I

Prepared on behalf of the
National Aeronautics and Space Administration

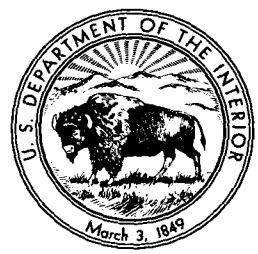

UNITED STATES GOVERNMENT PRINTING OFFICE, WASHINGTON : 1971

I

UNITED STATES DEPARTMENT OF THE INTERIOR

ROGERS C. B. MORTON, *Secretary*

GEOLOGICAL SURVEY

W. A. Radlinski, *Acting Director*

Library of Congress catalog-card No. 77-611770

For sale by the Superintendent of Documents, U.S. Government Printing Office
Washington, D.C. 20402 - Price 75 (paper cover)

CONTENTS

ILLUSTRATIONS

TABLES

GEOLOGY OF THE LUNAR CRATER VOLCANIC FIELD, NYE COUNTY, NEVADA

By David H. Scott and N. J. Trask

ABSTRACT

The Lunar Crater volcanic field in east-central Nevada includes cinder cones, maars, and basalt flows of probably Quaternary age that individually and as a group resemble some features on the moon. Three episodes of volcanism are separated by intervals of relative dormancy and erosion. Changes in morphology of cinder cones, degree of weathering, and superposition of associated basalt flows provide a basis for determining the relative ages of the cones. A method has been devised whereby cone heights, base radii, and angles of slope are used to determine semiquantitatively the age relationships of some cinder cones.

Structural studies show that cone and crater chains and their associated lava flows developed along fissures and normal faults produced by tensional stress. The petrography of the basalts and pyroclastics suggests magmatic differentiation at depth which produced interbedded subalkaline basalts, alkali-olivine basalts, and basanitoids. The youngest flows in the field are basanitoids.

All the features in the Lunar Crater volcanic field have analogs on the moon. Features on the moon interpreted as maars may have details of structure and composition similar to Lunar Crater itself. Erosion on the moon, probably caused by the impact of small particles and attendant downslope slumping of material, appears to be grossly similar to the erosion of the cinder cones in the Lunar Crater volcanic field, where removal of material by streams is at a minimum.

INTRODUCTION

The Lunar Crater volcanic field is in the southern part of the Pancake Range, Nye County, Nev. (fig. 1), and is crossed by U.S. Highway 6 about midway between the towns of Ely and Tonopah. Cinder cones, craters, and basalt flows cover an area of more than 100 square miles and represent the latest episode in the long eruptive history of this area. This volcanism is believed to have occurred during the late Quaternary.

Knowledge of volcanic cones, craters, and maars and the modification of their original forms by relatively "dry" erosional processes has a direct bearing on extraterrestrial research. The present study has been directed primarily toward obtaining quantitative data on the morphology of these volcanic features for the purpose of comparing them with structures on the moon which appear to be similar. Petrographic, stratigraphic, and structural studies of basalt flows, pyroclastic ejecta, and, to a lesser extent, ignimbrite and sedimentary sequences have provided information on age relationships, modes of origin, and the sequence of development of the cones, craters, and basalt flows.

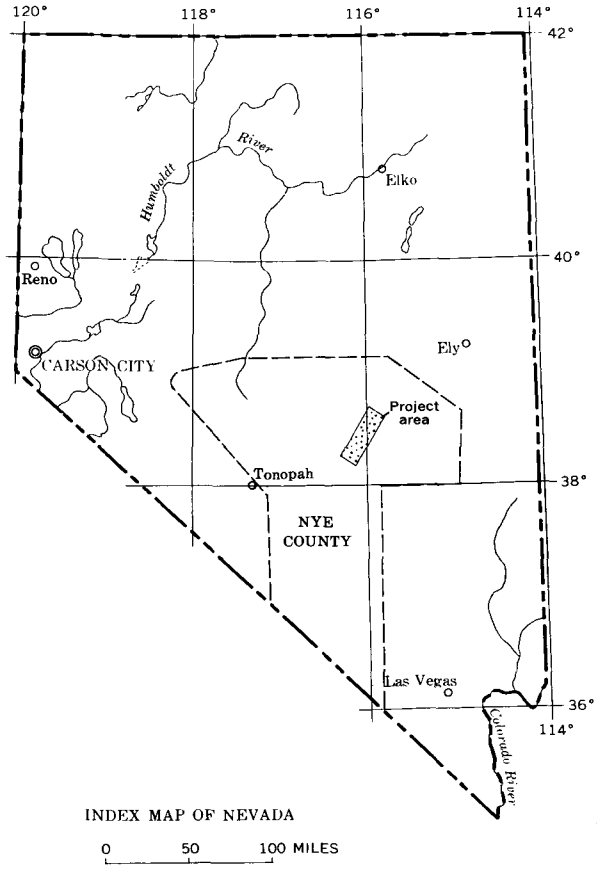

FIGURE 1.—Location of the Lunar Crater volcanic field.

Earlier work relevant to the Lunar Crater volcanic field includes a description of the basalts near Black Rock Summit by Vitaliano and Harvey (1965) and a description of ultramafic xenoliths in the basalts and pyroclastic ejecta by Trask (1969). A preliminary geologic map of Nye County, Nev., by Kleinhampl and Ziony (1967) shows the general structural and stratigraphic relationships between the Quaternary(?) volcanic flows and cinder cones and the surrounding Tertiary ignimbrites and Paleozoic sedimentary rocks. A more detailed study of the Tertiary ignimbrites is underway by the U.S. Geological Survey (Snyder and others, 1969).

ACKNOWLEDGMENTS

This report is part of a study of basaltic craters and lava fields done on behalf of the National Aeronautics and Space Administration under contract No. R-66. H. G. Wilshire of the Geological Survey visited the area with the authors and contributed ideas included in the manuscript. Professors C. A. Nelson, D. Carlisle, and K. D. Watson of the University of California at Los Angeles reviewed the fieldwork and parts of the manuscript.

GEOLOGIC SETTING

Quaternary(?) basalt flows, cinder cones, and craters occupy a high valley in the southern part of the Pancake Range and are underlain and partly surrounded by Tertiary ignimbrites, rhyolitic lava flows, and Paleozoic carbonate rocks.

The Tertiary ignimbrites compose the bulk of all deposits and are made up of 14 mappable sheetlike units with a cumulative thickness of about 8,000 feet. On the basis of the mineralogy of the phenocrysts, the ash-flow tuffs range from rhyolitic to andesitic and show the characteristic welded to nonwelded zonal patterns typical of simple cooling units described by Smith (1960). Some of the ash-flows appear to be correlative with ignimbrite units described by Cook (1965) which are of regional extent in eastern Nevada. Radiometric dating indicates that most of the ignimbrites were extruded during the Oligocene and early Miocene (Armstrong and others, 1969).

The Paleozoic sedimentary rocks consist primarily of dolomite, dolomitic limestone, and quartzite and have a combined thickness of about 4,000 feet. Five formations in the Ordovician, Silurian, and Devonian Systems have been identified; they also occur elsewhere throughout a large part of Nevada.

Structures in this region are relatively simple and are reflected by the physiography typical of the Basin and Range province. Folding, where present, is mild, and numerous normal faults separate blocks which are tilted generally eastward. In places this picture is made more complex by large masses of Paleozoic rocks that have slid over the Tertiary ignimbrites.

LUNAR CRATER VOLCANIC FIELD

Alkaline basalt flows and pyroclastic ejecta have been extruded from cratered cones, from mounds, and from fissures in a central area about 20 miles long and 5 miles wide. Many of these features occur along lineaments trending about N. 30° E. The cinder cones are composite structures made up of ash, lapilli, blocks, bombs, scoriaceous agglutinate, and flows of dense basalt. Some of the cones have diameters of about a mile with peaks or cratered rims more than 500 feet above their bases. Fragments of the underlying ignimbrites are present in and around the larger cones and are especially common in rim material at Lunar Crater, one of two maars in the area.

Evidence for recent volcanism and for the relative ages of flows, cinder cones, and maars was obtained from the degree of weathering and erosion, the stratigraphic and structural relationships, and the mineral alteration shown in thin sections of the basalts. The morphology of cones and the modification of original forms with time were objects of a special study wherein a quantitative method was developed for establishing relative age. The origin and sequence of events in the volcanic field were synthesized from field, photogeologic, and petrographic studies and from chemical analyses of the basalts.

DESCRIPTION AND AGE OF FLOWS, CINDER CONES, AND MAARS

The absolute age of the volcanism is not known, and the assignment of these rocks to the Quaternary (?) is tentative. Many of the flows and cinder cones appear to be young, possibly Holocene in age, as shown by:

1. Sharp contacts of basalt flows and ejecta aprons with valley alluvium and playa lake beds, and little accumulation of erosion products along flow and apron margins.
2. Absence of soil cover and vegetation on some flows and ejecta aprons.
3. Local flowage across fault scarps where recent faulting is suggested by topography.
4. Fresh-appearing black ash and lapilli overlying more weathered material on the rims of craters.
5. Sharp edges of grooves in blocks and the absence of a weathered surface layer on broken samples from some flows.
6. Steep profiles of some cones where the angle of slope of loose ejecta has been little affected by erosion and sliding.

7. The occurrence of cinder mounds on talus deposits accumulating near the bases of steep cliffs.
8. The intercalation of post-Lake Lahontan beds between ejecta layers. That these lake beds probably do not predate the intense pluvial periods and high shorelines of late Lake Lahontan time which reached maximum altitudes from 9,500 to 18,000 years ago (Morrison and Frye, 1965, p. 17–18) is suggested by the absence of any higher shorelines within the volcanic field.

The relative ages of basalt flows and pyroclastic materials forming cones are partly revealed by superposition, amount of weathering and erosion, degree of mineral alteration, and cone morphology. The flows and cinder cones have been placed in three relative age groups: older, intermediate, and younger; their distribution is shown on plate 1. In places the cratered and breached cones from which these flows issued are clearly visible, and their associated ejecta blankets are thus relatively dateable. Generally, however, pyroclastic materials merge imperceptibly over a wide area; except for more recent outbreaks of cinders which appear as color contrasts around some crater rims, the relative ages of cones are best determined by comparative morphologies. Volcanism was intermittent, and periods of quiescence are marked by weathered zones between flows and by soil development between cinder deposits on the sides of some cones. These periods of dormancy appear to have been geologically brief and locally restricted.

FLOWS AND CONES OF OLDER AGE

The surfaces of older flows are smooth, highly weathered, coated by desert polish, and mostly covered with thin sandy soil and sparse to abundant vegetation. In places the flows are tilted and cut by faults which were later covered by flows of intermediate age (pl. 1). In various parts of the area, the older flows rest directly upon ash-flow tuffs. No pyroclastic material is directly associated with the older basalts, but some low-relief, deeply gullied, highly infilled cratered cones are of advanced age and may have been formed during this earlier period of volcanism. One of these older cratered cones (profiles *R–R′*, *S–S′*, fig. 7) is partly filled with alluvium and has outbreaks of flows of intermediate age on its rim and flanks.

FLOWS AND CONES OF INTERMEDIATE AGE

Basalt flows and cinder cones of intermediate age are the most widespread of all the deposits and extend from the northern to the southern edge of the volcanic field. The flows are classified according to the amount of weathering and erosion they have undergone, the amount of vegetation and sand that cover them, their position in sequence, and the degree of alteration of microphenocrysts in their groundmass. The cones of intermediate age exhibit a variety of sizes and shapes and are the most difficult structures of all the age groups to categorize. Generally they are moderately rilled and gullied and have rounded rims, and their craters are partly infilled. Their angles of slope, however, are quite variable, and a general trend showing a decrease in slope with age only becomes apparent when selected cones are carefully studied and further subdivided by relative age (fig. 8). In several localities the cones and their aprons are overlain by basalt flows of intermediate age; fluid lavas mark the final stages of eruption from these cones and have partly destroyed cinder cone walls during their extrusion. This criterion, however, is not always valid for establishing the eruptive sequence of flows and pyroclastic ejecta; some basalt flows seem to be partly covered by cones and may be older than the cones or the flows may have issued from vents and fissures beneath the blanketing pyroclastic material and would thus be younger than the cones. The maars of Lunar and Easy Chair Craters (figs. 2, 3) were formed during this intermediate period of volcanism.[1] The vent of Lunar Crater is about 3,800 feet in diameter and has penetrated basalt flows of older and intermediate age, but the ejecta are covered in places by pyroclastic material and flows also assigned to the intermediate age group. Basalts of intermediate age are exposed in the walls of Easy Chair Crater, but here the cinder cone source of these flows overlaps and has partly destroyed the northern rim of the maar.

FLOWS AND CONES OF YOUNGER AGE

The younger basalts and pyroclastics include several flows and cinder cones (fig. 4) covering an area of about 2 square miles, 1 mile north of U.S. Highway 6 and 3 miles east of Lunar Crater road. The basalt flows breached the walls of a prominent cinder cone on the west side of the volcanic field (cone profile *L–L′*, fig. 7). This cratered cone is considered to be the youngest large cinder cone in the volcanic field. There is little infilling of the crater, and the flanks of the cone are not gullied by erosion. The rim has remained relatively sharp, and loose ejecta form a slope of 35°, a maximum for cones in this area. The flows, only moderately viscous, were deflected around the base of an adjacent cone and formed two coalescing lobes on the valley floor. They are extremely rough and conspicuously black. The flows lack vegetation and rest upon basalts of older and intermediate age. The basalt surface has large arcuate ridges

[1] Maars are morphologically distinguished from volcanoes by having flat floors lying below the level of adjacent terrain and low, subdued rims. For a more complete discussion of maars in general, see Shoemaker (1962).

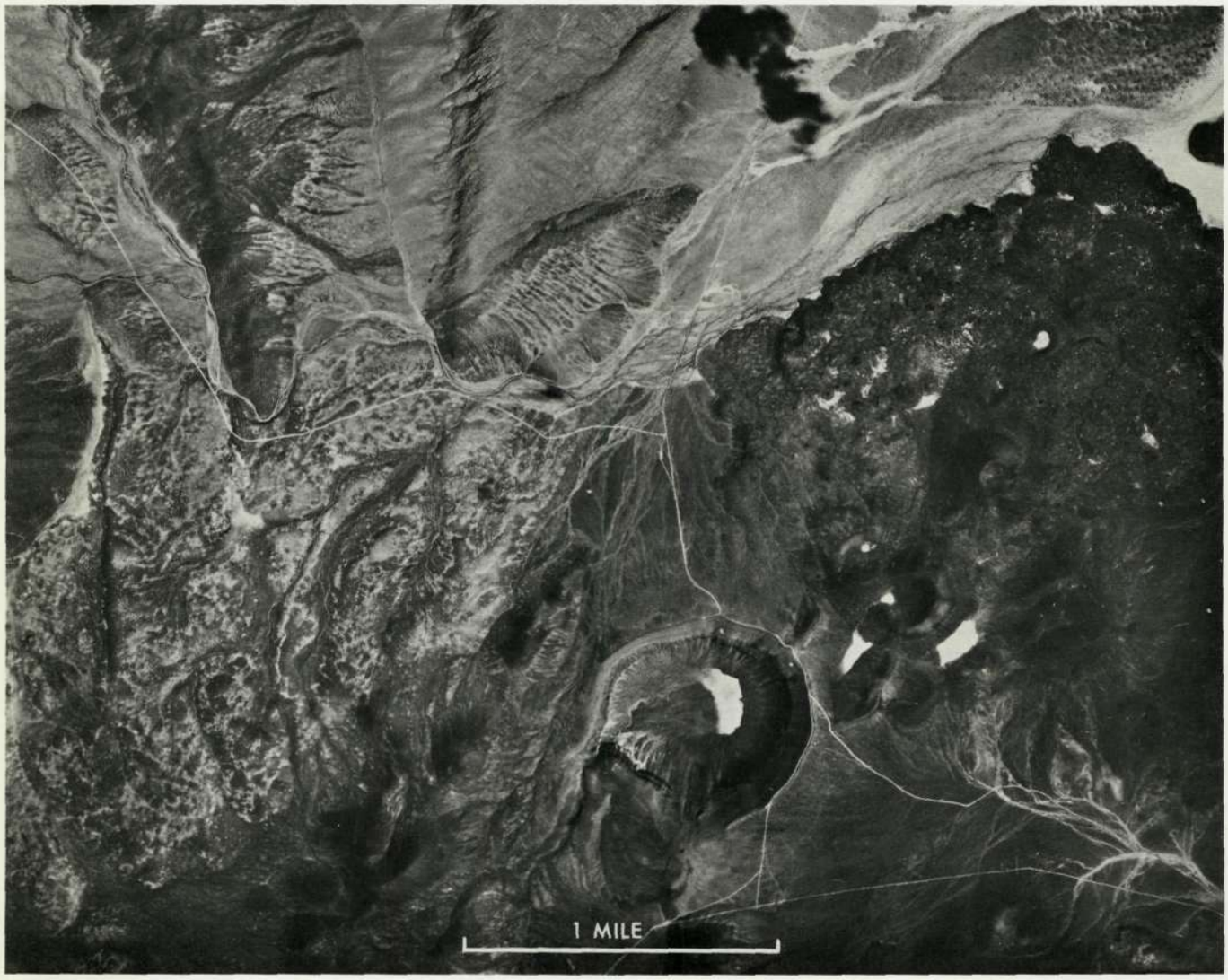

FIGURE 2.—Lunar Crater, lower right, 3,800 feet across. North is at top in all figures of both earth and moon. Deposits of normal cinder cone to northeast overlap the distinctive rim deposits of Lunar Crater.

convex in the direction of flow. The lava attained some rigidity during transport, and many of the broken blocks are deeply grooved and striated. Masses of autobreccia, measuring 10 feet on a side, were formed during the disruption of the moving mass as the surface and margins congealed.

Several miles to the east and immediately south of U.S. Highway 6 near Black Rock Summit, numerous small cinder mounds occur on talus deposits of ash-flow tuffs at the base of steep cliffs. These ejecta mounds are of recent origin and may be as young as, or younger than, the fresh-looking black basalts.

PYROCLASTICS AND MAAR DEPOSITS

Pyroclastic ejecta of the cinder cones and their aprons are generally similar throughout the volcanic field. Angular scoriaceous cinders, in varying shades of black, dark-gray, and red, interspersed with ropy, spindle-shaped and flattened bombs, form a loose accumulation on and around the cones. Ejecta associated with the younger basalts and some ejecta of intermediate age contain abundant fragments of olivine, plagioclase, and pyroxene; mafic and ultramafic xenoliths occur in the cores of bombs around two cones. Fragments of Tertiary ignimbrites are not uncommon in the pyroclastic material forming the larger cones. A small piece of granite containing garnets was found in a bomb associated with an older basalt flow; no rocks of this sort are exposed in the southern Pancake Range.

Rim material at the maars of Lunar and Easy Chair Craters is made up of outward-dipping coarsely bedded loose to consolidated palagonite tuff and subangular

FIGURE 3.—Easy Chair Crater, at bottom, 1,600 feet across in east-west direction. Floor only slightly lower than surroundings, overlapped by cinder cone on north side.

fragments of country rock up to boulder size. At Lunar Crater a large amount of ignimbrite and basalt torn from the walls of the crater is included in the ejecta, but ignimbrites are not so common at Easy Chair Crater. At this locality, abundant accumulations of crystal fragments are mixed with loose material around the flanks of the crater and in some indurated breccias exposed in the walls of the vent. No Paleozoic carbonate rocks were found in ejecta from either the maars or cinder cones.

PETROGRAPHY

Most of the flows are vesicular and porphyritic. Phenocrysts of olivine, plagioclase, pyroxene, and opaque minerals are set in a fine-grained to glassy brown to black groundmass. Chemical analyses (table 1) show that the basalts fall within the alkaline basalt field on the alkali-silica diagram for Hawaiian rocks (fig. 5) (MacDonald and Katsura, 1964, fig. 1). Modal olivine exceeds 5 percent in many of the basalts, and normative nepheline is greater than 5 percent in half the samples for which normative minerals have been calculated (table 1). The analyses show that the lavas range from subalkaline basalts (SiO_2=48–50 percent, normative nepheline=0 percent, normative hypersthene>0 percent), to alkaline olivine basalts (SiO_2=46–48, normative ne=0–5 percent), to basanites or basanitoids (SiO_2<46 percent, normative ne>5 percent, modal ne=0 percent).

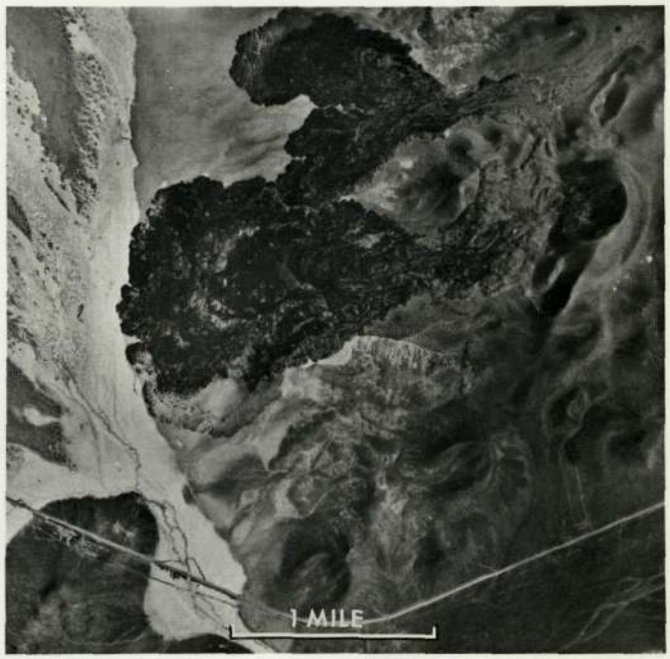

FIGURE 4.—Very fresh appearing black basalt flows north of U.S. Highway 6.

OLDER FLOWS

The older basalts contain microphenocrysts of highly corroded plagioclase and olivine. In some rocks the olivine is almost completely altered to "iddingsite." Basal basalt flows exposed in the walls of Lunar Crater rest upon ash-flow tuffs and contain large phenocrysts of plagioclase and small amounts of olivine. These flows (1, table 1) are similar in their high silica content to early flows south of Lunar Crater (2, table 1). In some locations, low viscosity and high temperature are suggested by contorted ropy structures and the relative sparsity of vesicles.

INTERMEDIATE FLOWS

Although fine distinctions cannot be made between the degree of mineral alteration shown in thin section and the relative ages of flows, plagioclase and olivine appear comparatively fresh in basalts of intermediate age. Relative age groupings of 13 samples made on the basis of mineral alteration agree with their classification as either older or intermediate age made on the basis of other criteria. The uppermost flows in the walls of Lunar Crater are of intermediate age and contain olivine phenocrysts and little visible plagioclase. Here, as elsewhere in the area, basalts of intermediate age contain less silica and more normative nepheline than the older flows (table 1). Ultramafic and mafic xenoliths are common in flows of intermediate age near Easy Chair Crater.

TABLE 1.—*Bulk chemical analyses and molecular norms of basalt from Lunar Crater volcanic field*

[Analyst: C. L. Parker]

	1	2	3	4	5	6	7	8	9	10
Chemical analyses [Weight percent]										
SiO_2	48. 46	49. 59	47. 67	47. 24	47. 76	44. 79	44. 37	44. 88	44. 66	44. 41
Al_2O_3	16. 19	18. 01	14. 55	16. 52	15. 29	15. 27	15. 65	15. 60	15. 35	15. 45
Fe_2O_3	6. 60	5. 47	5. 41	3. 38	5. 98	4. 21	4. 44	4. 29	3. 39	2. 74
FeO	6. 30	4. 88	6. 45	8. 75	6. 84	8. 12	7. 94	7. 47	7. 92	8. 66
MgO	5. 17	4. 28	9. 37	6. 30	6. 53	8. 75	7. 80	7. 76	8. 96	8. 74
CaO	8. 37	9. 71	9. 06	8. 42	9. 06	10. 02	9. 62	9. 94	10. 40	10. 49
Na_2O	3. 78	2. 81	3. 05	4. 15	3. 45	3. 51	4. 32	4. 13	3. 67	3. 99
K_2O	1. 25	1. 17	1. 00	1. 52	1. 16	1. 11	1. 88	1. 83	1. 84	1. 80
H_2O+	. 14	. 43	. 34	. 12	. 14	. 41	. 22	. 11	. 16	. 11
H_2O-	. 15	. 76	. 27	. 06	. 10	. 21	. 17	. 13	. 04	. 01
TiO_2	2. 73	1. 88	1. 84	2. 40	2. 57	2. 65	2. 43	2. 44	2. 33	2. 34
P_2O_5	. 49	. 54	. 33	. 51	. 48	. 52	. 74	. 73	. 65	. 73
MnO	. 18	. 15	. 18	. 19	. 18	. 19	. 22	. 21	. 21	. 22
CO_2	. 05	. 10	. 28	. 19	. 27	. 03	. 08	. 03	. 07	. 04
Cl	. 00	. 01	. 00	. 04	. 02	. 03	. 04	. 06	. 07	. 05
F	. 06	. 07	. 04	. 06	. 06	. 07	. 09	. 08	. 08	. 08
Cr_2O_3	. 01	. 01	. 05	. 02	. 03	. 03	. 03	. 04	. 06	. 06
NiO	. 01	. 00	. 03	. 01	. 01	. 02	. 02	. 02	. 03	. 03
Subtotal	99. 94	99. 87	99. 92	99. 88	99. 92	99. 93	100. 06	99. 75	99. 89	99. 95
Less O	. 03	. 03	. 02	. 04	. 03	. 04	. 05	. 04	. 05	. 04
Total	99. 91	99. 84	99. 90	99. 84	99. 90	99. 90	100. 01	99. 71	99. 84	99. 91
C.I.P.W. norms [Weight percent]										
Q	0. 00	5. 09	0. 00	0. 00	0. 00	0. 00	0. 00	0. 00	0. 00	0. 00
or	7. 39	6. 92	5. 91	8. 99	6. 86	6. 56	11. 10	10. 84	10. 89	10. 63
ab	32. 00	23. 73	25. 84	26. 50	29. 07	17. 98	12. 60	13. 85	10. 33	8. 24
an	23. 53	33. 15	23. 08	22. 14	22. 90	22. 76	17. 81	18. 91	20. 27	19. 12
ne	. 00	. 00	. 00	4. 53	. 00	6. 24	12. 80	11. 24	10. 97	13. 62
di	11. 36	8. 50	14. 20	12. 24	13. 60	18. 62	19. 51	20. 40	21. 31	22. 45
ol	. 41	. 00	9. 48	14. 14	4. 10	14. 60	12. 50	11. 61	14. 69	15. 26
mt	9. 58	7. 94	7. 85	4. 91	8. 68	6. 11	6. 43	6. 24	4. 92	3. 97
il	5. 18	3. 58	3. 50	4. 56	4. 88	5. 04	4. 61	4. 65	4. 43	4. 44
ap	1. 16	1. 28	. 78	1. 21	1. 14	1. 23	1. 75	1. 73	1. 54	1. 73
hy	8. 90	8. 27	8. 01	. 00	7. 78	. 00	. 00	. 00	. 00	. 00

1. Older basalt, subalkaline (LC-51); lowermost flow in Lunar Crater, collected from north wall, 500 ft south of cairn. (Sample locations shown on pl. 1.) Light gray, with phenocrysts of plagioclase (up to 5 mm) and olivine (avg 1 mm) in groundmass of plagioclase, olivine, and opaque minerals.
2. Older basalt, subalkaline (LC-101); 30 ft above contact with Tertiary ignimbrite in canyon 2 miles south of Lunar Crater. Light gray, with abundant plagioclase phenocrysts (up to 3 mm) and phenocrysts of olivine (avg 0.5 mm) in groundmass of plagioclase, olivine, opaque minerals, and glass.
3. Older basalt, subalkaline (LC-95); from middle of sequence in Lunar Crater, collected from northwest wall, 1,000 ft southwest of cairn. Medium gray, vuggy, with phenocrysts of olivine (up to 2 mm) and plagioclase (up to 3 mm), rare xenocrysts(?) of clinopyroxene (up to 2 mm) in groundmass of plagioclase, olivine and opaque minerals.
4. Older basalt, alkalic (LC-109); from vegetated flow, 1,700 ft north of fresh black basalt (younger basanitoid) and 2.5 miles north of U.S. Highway 6. Dark gray with phenocrysts of plagioclase, olivine, and clinopyroxene (avg 0.5 mm) in groundmass of plagioclase, clinopyroxene, opaque minerals, and glass.
5. Basalt of probable intermediate age, subalkaline (LC-99) 2.5 miles south of Lunar Crater. Light purplish gray, with phenocrysts of plagioclase, olivine and clinopyroxene (avg 2 mm) in groundmass of plagioclase, clinopyroxene, olivine, and opaque minerals.
6. Basanitoid of intermediate age (LC-54); near top of sequence in Lunar Crater, collected in gulley at southwest corner. Dark gray, with phenocrysts of olivine and clinopyroxene (avg 1.0 mm) and microphenocrysts of plagioclase in groundmass of plagioclase, clinopyroxene, olivine, opaque minerals, and glass.
7. Basanitoid of intermediate age (LC-61); lightly vegetated flows 1.6 miles northeast of Lunar Crater. Black, highly vesicular, with xenocrysts of clinopyroxene (up to 5 mm) in groundmass of plagioclase, clinopyroxene, olivine, opaque minerals, and glass.
8. Basanitoid of intermediate age (LC-111); uppermost flow 0.5 miles northeast of Easy Chair Crater. Black, with ultramafic xenoliths (up to 5 cm) and xenocrysts of olivine, clinopyroxene, and plagioclase (up to 5 mm) in groundmass of plagioclase, clinopyroxene, olivine, opaque minerals, and glass.
9. Younger basanitoid (LC-9); from unvegetated, rough black flows north of U.S. Highway 6. Black, vesicular, with ultramafic xenoliths (up to 15 cm), and xenocrysts of olivine, clinopyroxene, and plagioclase (up to 8 cm) in groundmass of plagioclase, clinopyroxene, olivine, opaque minerals, and glass.
10. Younger basanitoid (LC-48); from unvegetated, rough black flows, 0.25 miles west of largest cinder cone in cluster just north of U.S. Highway 6. Description same as 9.

YOUNGER FLOWS

The younger flows and pyroclastic rocks north of U.S. Highway 6 are similar in chemistry and mineralogy to the flows of intermediate age and are exceptionally rich in ultramafic xenoliths and in xenocrysts of olivine, pyroxene, and plagioclase. The xenoliths, which range in size from microscopic to several inches, are generally rounded and have widely variable compositions and textures. Lherzolites are moderately to strongly deformed; olivine-rich wehrlites and dunites are intensely deformed; clinopyroxenites, clinopyroxene-rich wehrlites, and gabbros are undeformed to only slightly deformed. The lherzolite probably came from the upper mantle. The clinopyroxene-rich wehrlite and

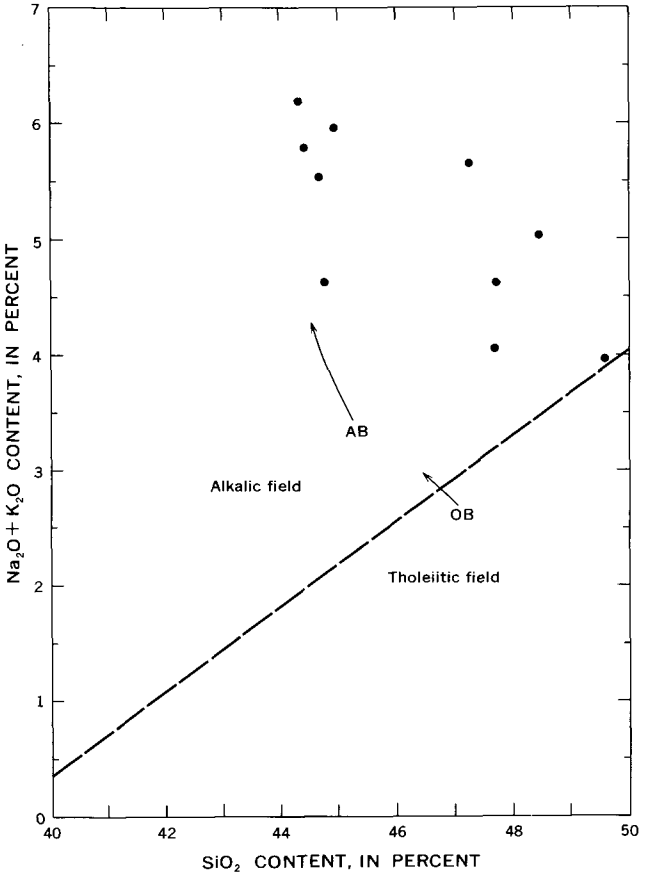

FIGURE 5.—Alkali-silica diagram showing variations in compositions of rocks given in table 1. Alkalic-tholeiitic field boundary from MacDonald and Katsura (1964, fig. 1). Arrows indicate fractionation trends determined experimentally by Green and Ringwood (1967) at high pressures (13–18 kb) for alkali olivine basalt composition (AB) and olivine basalt composition (OB) (mixture of alkali olivine basalt and olivine tholeiite).

clinopyroxenite may be cumulates from the magma that produced the older and intermediate age basalts; the source of the highly deformed olivine-rich wehrlite and dunite is not clear. The abundance of inclusions in these flows may have affected their bulk chemical analyses (9, 10, table 1), but the flows are chemically similar to basanitoids of intermediate age which do not have noticeable xenoliths (6, 7, table 1).

STRUCTURE

Tertiary ignimbrites exposed in cliffs around the basalt flows and cinder cones are useful markers for determining geologic structure. Normal faulting is prevalent throughout the tuff sequence and dominates the structural history from middle-Tertiary time. Of the several hundred faults mapped, only a few are demonstrably of pre-Miocene age. On an equal-area basis, the Quaternary(?) volcanic field is relatively unfaulted; however, cone chains, fissures, and faults follow the major northeast-southwest trend of faulting and jointing in the ignimbrites (fig. 6). Near Black Rock Summit large masses of Paleozoic rocks, emplaced by gravity sliding, overlie ash-flow tuffs.

ORIGIN AND ERUPTIVE HISTORY OF BASALT FLOWS, CINDER CONES, AND MAARS

Basalt flows, cinder cone chains, mounds, craters, and fissures rimmed with pyroclastic ejecta were produced along normal faults and lineaments of tensional stress which became active during the Miocene Epoch and which continued being active throughout the Quaternary Period. At least three episodes of late volcanism occurred throughout the volcanic field; they were separated by brief periods of relative dormancy. These interludes may not have been distinct and probably represent overlapping pulses of activity. Each episode began with the eruption of pyroclastic material that formed small mounds; as these grew larger and became cone shaped, the initial extrusion of highly vesicular basalt flows and ejection of fragments produced composite or mixed volcanic structures. This early explosive phase probably resulted from a combination of the high volatile content of the magma with violent gas loss and of the greater amount of ground water available at the onset of volcanism. In the final stages, as magma continued to rise in the vents, many cones were breached where the lavas overflowed or eroded the walls of cinders and ashes. The weakness of the ringwalls was apparently conditioned by linear fissures and faults along which the cones developed, as shown by the preferred northeast-southwest orientation of the ruptures. A similar sequence of eruptive activity along linear fissures is described by Rittmann (1962, p. 88–91) for the Threngslaborgir line craters.

In more extreme cases, the rapid breaking through of magmatic gases and (or) phreatic steam has resulted in the explosive discharge of fragmentary material with little or no lava. Because of the high velocity of the escaping gases, ejecta were deposited as low rim-forming breccias around vents of such craters as Lunar and Easy Chair Craters. These maars have deep flat floors lying below the level of adjacent valleys. Outer slopes are gentle and do not exceed 15° at Lunar Crater. The coarsely bedded ejecta, made up of palagonite tuff, lapilli, and country rock, dip outward from the vent at low angles; underlying basalt flows and ignimbrites are not deformed. The vents of maars are characteristically funnel shaped (Shoemaker, 1962), and the apparent absence of Paleozoic carbonate rocks in the rim material may be attributed to the rapid narrowing of the vent with depth and the consequent smaller volume

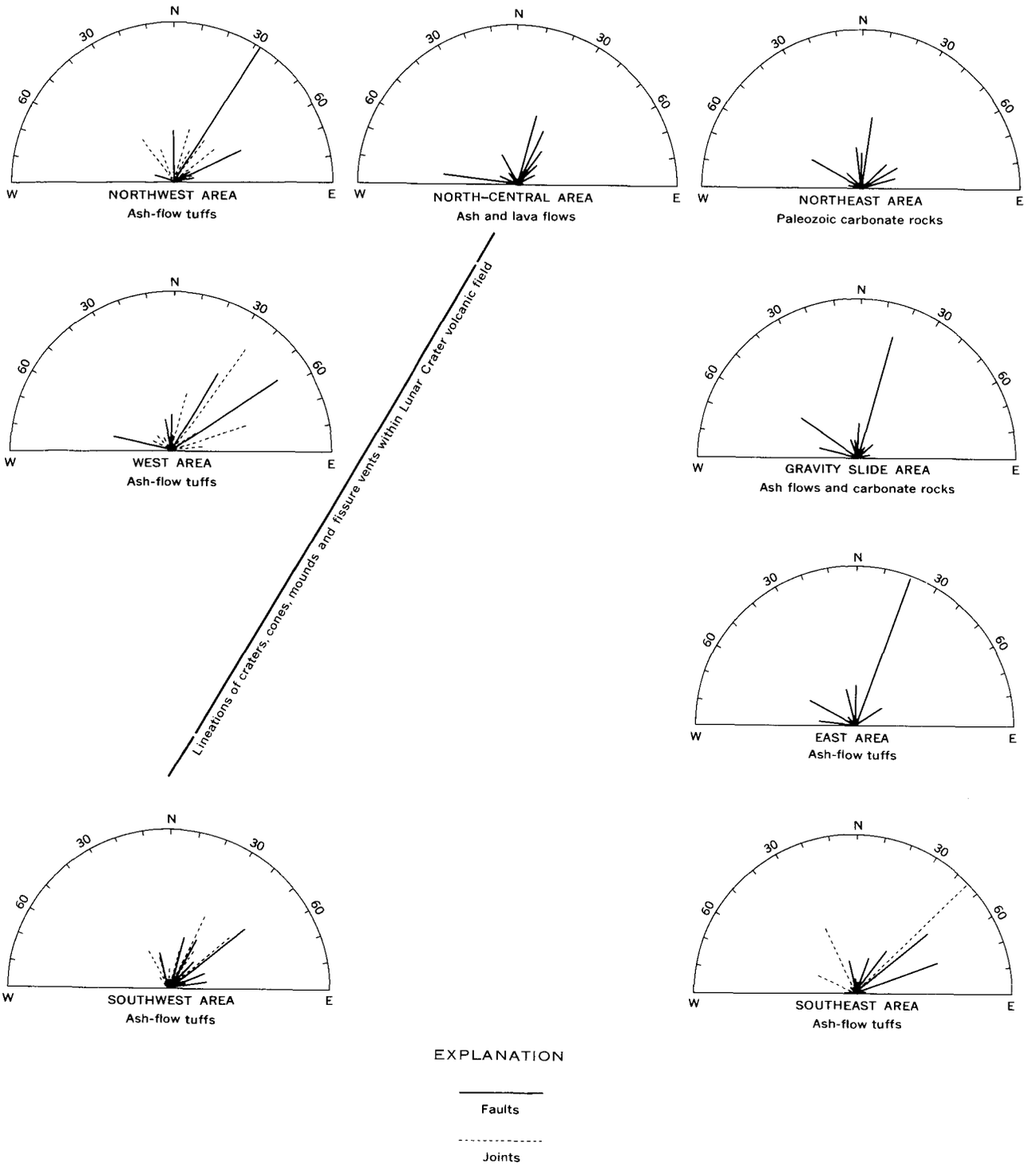

FIGURE 6.—Trends of fault and joint systems in the Lunar Crater volcanic field and vicinity. Radius of rose diagrams is approximately 50 percent of number of faults and joints; the average number of faults per sector is 40.

of deeper country rock ejected. This idea is also suggested by the larger amount of younger ignimbrites appearing in rim material of the maars than in cinder cones. On the other hand, a violent discharge of volatiles may not have originated or extended below a depth of about 6,500 feet, the estimated thickness of ignimbrites overlying Paleozoic rocks in the Lunar Crater area. The nonwelded zones of these tuffs are highly porous water reservoirs of low permeability. Intrusions of magma into these beds might have caused sudden vaporization of water and steam blast explosions, provided the rate of heat accumulation exceeded the rate at which heat was lost by movement of ground water through the ash flows. However, the Paleozoic carbonate rocks have little porosity, and their depth of burial, below about 6,000 feet, is such that the critical pressure of water is exceeded by the hydrostatic pressure; therefore, steam cannot form (Rittmann, 1962, p. 50).

Whether the maars of Lunar and Easy Chair craters resulted from steam blast or rapid discharge of magmatic gases, their uniqueness in the cinder cone field is not readily explainable. Some evidence suggests that, in the underlying ignimbrites, the maars occupy a structurally low position that would favor the accumulation of subsurface water. The proximity of cinder cones both older and younger than the maars, however, indicates that other factors have probably been more important. The location of the craters and cones along faults and lineaments parallel to major fault systems precludes an origin due to the flow of basalt over ponded water or marshy grounds; thus they are not similar to the pseudocraters of the Icelandic type described by Thorarinsson (1953).

The flows in the Lunar Crater volcanic field consist of interbedded subalkaline basalts, alkali olivine basalt, and basanitoids. (See section on "Petrography".) The lower and middle flows of the basalt sequence exposed in the walls of Lunar Crater consist of subalkaline basalt (1, 3, table 1) and the uppermost flow of basanitoid (6, table 1). The youngest flows in the field are basanitoids. Removal of aluminous pyroxenes from relatively olivine-rich magmas at moderate to high pressures (13–18 kb; 40–60 km) can account for these trends of increasing alkalis with decreasing silica (Green and Ringwood, 1967; MacDonald, 1969). The lavas in the Lunar Crater field are higher in alkalis as a whole than those in Hawaii (fig. 5) on which the experimental results of Green and Ringwood (1967) are based, and thus do not fall exactly on the fractionation trends shown in their diagrams. A subcrustal magma chamber may have existed under the Lunar Crater area in which subalkaline basalt magma underwent differentiation by removal of aluminous clinopyroxene with or without alumininous orthopyroxene to produce a basanitic magma. Tapping of the magma chamber at intervals would result in extrusion, alternately, of subalkaline lava and basanitic lava; thus, the two types would become interbedded. The feldspar-rich, quartz normative lava (2, table 1) could be formed by separation of olivine and clinopyroxene at depths of 15–35 km (Green and Ringwood, 1967, p. 157). Xenoliths of clinopyroxenite and clinopyroxene-rich wehrlite in relatively young flows in the Lunar Crater area are undeformed and have textures suggesting that they formed as cumulates (Trask, 1969). They may be representative of these possible high-pressure differentiates. No orthopyroxene has been noted in any ultramafic xenoliths that are interpreted as cumulates.

Quaternary basaltic rocks, chemically similar to those in the Lunar Crater volcanic field, are present in the Mojave Desert area of southeastern California (Wise, 1969; Smith and Carmichael, 1969). These rocks range from subalkaline basalts with 4 percent total alkalis to basanites with 5–6 percent total alkalis. In this area, however, the trend seems to be from basanites in the older flows to subalkaline basalts in the younger flows. Wise (1969) postulates a model for magma generation in which continuous partial melting occurs and the melt moves upward into zones of successively lower pressures. The mechanism of magma generation seems to have been quite different there than at the Lunar Crater volcanic field.

QUANTITATIVE STUDIES OF CINDER CONES IN LUNAR CRATER VOLCANIC FIELD

GROWTH AND EROSION OF CONES

In the first stages of volcanism, small mounds of cinders formed with convex external slopes of about 10° or less; several never developed beyond this state. As eruption proceeded, some mounds grew larger and became cone shaped. Their concave slopes averaged about 25° but some were as much as 35°. Some of these cones attained heights of 500–600 feet (fig. 7). The loose accumulation of ash and lapilli formed highly porous and permeable layers in the cone structure. Erosion of such material by rainfall is much slower than erosion of more consolidated material. Even so, the cones were eventually worn down by erosion and gravity sliding of loose material so that concave profiles were accentuated in the early stages of their history. The upper parts of the steeper slopes of the cones became channeled by numerous small rills, while their lower parts were gullied by flood streams carrying greater loads of material. Craters became partly infilled and their rims more rounded as erosion proceeded.

420-710 O - 71 - 2

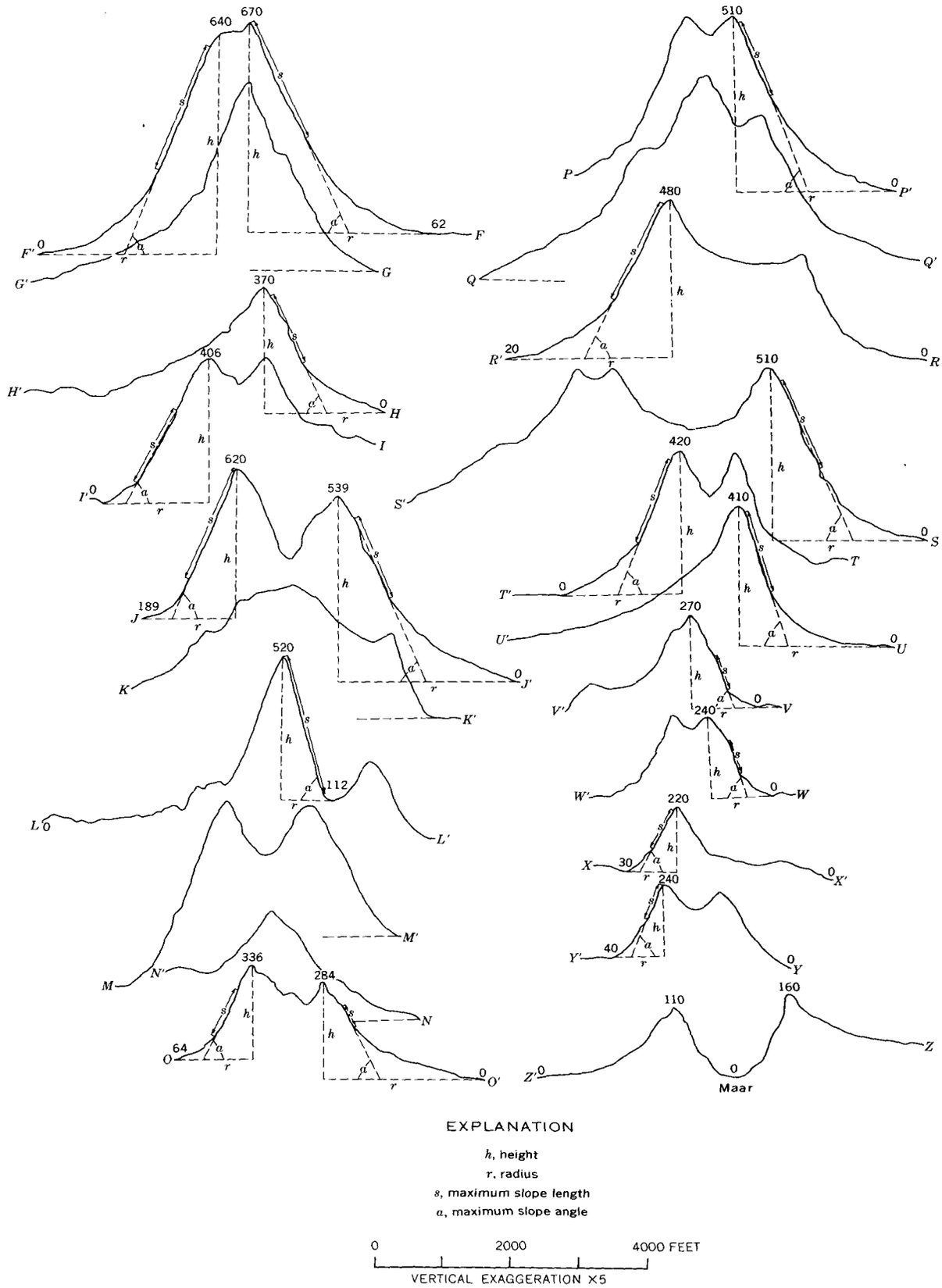

FIGURE 7.—Profiles of selected cinder cones in the Lunar Crater volcanic field. (See pl. 1 for locations.) Elevations are in feet above lowest point on profile. Profiles determined by J. D. Crossen, U.S. Geological Survey.

MORPHOLOGY AND AGE

Comparisons of their morphologies allow the assembly of cones into relative age groups. Features considered are—

1. Rill development on the upper flanks of cones.
2. Gully dissection of cone bases.
3. Erosive modification of crater rim—from sharp to partly rounded to well worn with low relief.
4. Relative ages of basalt flows associated with cones.
5. Influence of ejecta aprons on drainage pattern—or, conversely, the destruction of arcuate peripheral aprons by stream fill and channeling.
6. Infilling of craters.
7. Relative area proportions of cone aprons to central prominence.
8. Distinctive color changes produced by more recent ejecta around rims of craters, a variation which shows reconstruction of an older surface by later eruptions.
9. Parasitic cone development.

With the exception of 4, 8, 9, these features represent morphological changes by erosive processes (mainly mass transport by running water) which might be quantified. All the cones are uniform in composition and particle size and are generally similar in shape. Thus duration of exposure is the only variable that has influenced their gradual modification and eventual destruction in an area of equal rainfall. Preliminary attempts to assign numerical values to such features as rill and gully development or sharpness versus roundness of crater rims were successful enough to allow arranging the cones into assemblages of three relative age groups. This quantification method is restricted because of lack of knowledge as to how to weight the variables. If carried too far, conflicts arise, and relative age discrepancies become apparent. In the final analysis, the most satisfactory method resulted from individual comparisons of cone pairs and the grouping and regrouping of these combinations until a fair degree of relative age order was established.

Theoretically, the angle of repose of the unconsolidated cinders and lapilli is greatest at the time that they are first deposited. Slopes decrease thereafter by erosion of the summit and flanks of a cone. The length of maximum slope along the upper part of the cone profile becomes modified with age. The summit is rounded, and the base filled upward and outward by the downward transport of material. The line of maximum slope decreases to an inflection point, and all slopes become less than the angle of repose of the material. The angle of slope, as well as the relative length of the line of maximum slope, compared, say, to the height of the cone might provide an index ratio of age.

During the erosion process the base of a cone increases in width as the height decreases. This fact is particularly true in the Lunar Crater volcanic field, where rainfall is low and no permanent streams are present to carry away the products of erosion. For this reason, the changing cone retains a nearly constant volume, and the height and radius of the base are dependent variables that decrease and increase, respectively, with time.

MEASUREMENTS

Profiles of selected cones were prepared from aerial photographs by means of a mechanical profile tracer on a Kelsh plotter. Cone heights (h), base radii (r), lengths of maximum constant slopes (s), maximum slope angles (a), and the ratios r/h and s/h were determined from 18 profiles of cones (table 2). Figure 7 shows the method used for measuring h, r, s, and a of each cone; all measurements are reduced to true scale in table 2. It will be noted that r is not the half width of a cone but rather the horizontal distance from the rim prominence to the base of the cone apron; similarly, h represents the height of the rim above this horizontal base. In most places the actual width of a cone cannot be determined exactly from the profiles because of modifications of the flanks by basalt flows and parasitic outbreaks, and because of the interference of cone development by adjacent cones. By selecting h and r in this manner, the effect of cone destruction by breachment is minimized. The angle a is measured with respect to the horizontal.

TABLE 2.—*Dimensions of cones and relative age estimates from morphology*

Profile	Cone radius (r) (ft)	Cone height (h) (ft)	Length maximum slope (s) (ft)	Maximum slope (a) (degrees)	r/h	s/h	Relative age [1] (1, oldest)
F–F′	2,750	608	850	23	4.5	1.4	4
	2,600	640	790	26	4.1	1.2	
H–H′	1,750	370	485	23	4.7	1.3	3
I–I′	1,500	420	585	21	3.6	1.4	
J–J′	1,350	431	760	26	3.1	1.7	4
J–J′ [2]	2,600	539	540	26	4.7	1.0	
L–L′	760	408	685	35	1.9	1.7	6
O–O′	1,170	272	360	22	4.3	1.3	2
O–O′ [2]	2,280	284	140	22	8.0	.5	
P–P′	2,850	510	450	26	5.6	.9	2
R–R′	2,450	460	760	21	5.3	1.6	1
S–S′	2,950	510	600	24	5.8	1.2	
T–T′	1,750	420	530	26	4.1	1.2	3
U–U′	2,100	410	455	30	5.1	1.1	
V–V′	935	270	195	29	3.4	.7	5
W–W′	820	240	155	33	3.4	.7	
X–X′	780	190	280	22	4.1	1.5	4
Y–Y′	760	200	165	33	3.8	.8	

[1] Cones 1–5 associated with basalt flows of intermediate age. Cone 6 associated with basalt flow of younger age.
[2] Modified profile—old and young cone combination.

RESULTS AND SOURCES OF ERROR

Figure 8 shows a plot r/h, s/h, and a against relative morphological age. Values obtained from different profiles across the same cone are plotted individually. Average values for cones of the same age group having both

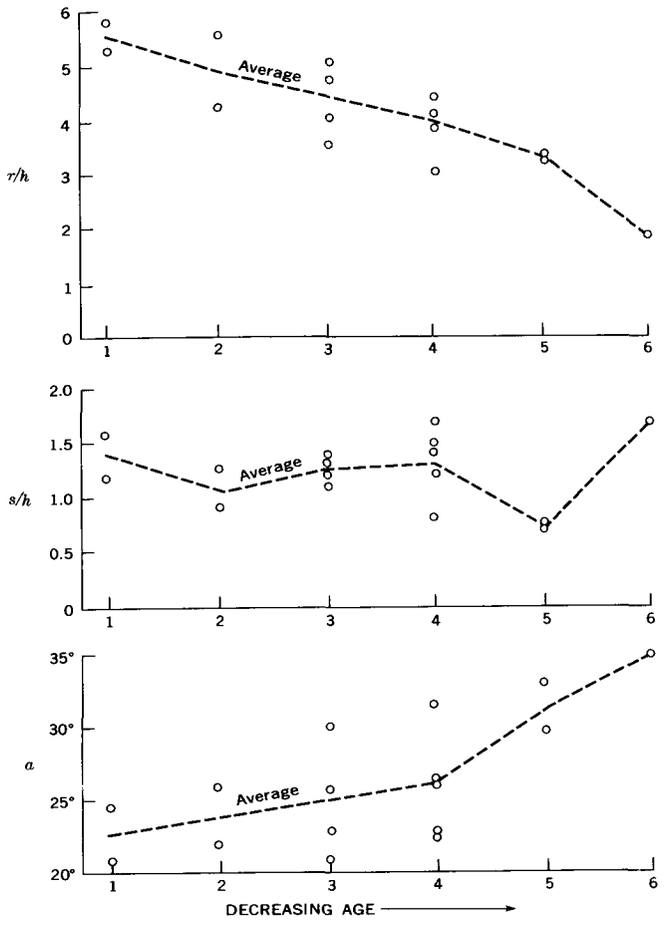

FIGURE 8.—Parameters indicating morphologies of cinder cones plotted against relative age. Parameters same as in table 2 and figure 7.

single and double profiles are obtained by using the double profile average as a single value. The positions of the profiles are shown on plate 1. It is apparent that direct relationships exist between r/h, a, and the relative ages of the cones. As would be expected, the ratio r/h increases with age, while a, the slope, decreases. The relation between s/h and age is erratic, and the reason for this is not clear. The difficulty may lie in that the linearity of a cone flank is more or less maintained with time even through the height and slope of the cone decrease.

Several factors influence theoretical concepts of age and morphology of cones:

1. Climate and physiography—differences in rainfall, temperature, wind velocity, stream runoff, load, and drainage are unimportant in this relatively small area of closed drainage and nearly equal elevation.
2. Duration of volcanism—parasitic cones, later eruptions from the same vent, and basalt flows directly influence the morphology of cones or, by their proximity, retard the spread of base material but may not completely destroy morphological evidence of actual age.
3. Internal structure—basalt flows and consolidated breccias interbedded with loose pyroclastic layers alter natural profiles and change erosion rates.
4. Cratering, breaching, and faulting of cones—if cone wall is weak and craters or breached craters destroy large parts of the upper walls of a cone, then the cone shape becomes irregular and cannot be accurately determined.
5. Size of original cone—large cones erode more slowly than smaller ones because the surface area receiving rainfall is proportionately less with respect to their volume. Thus, the assumption that geometrically similar cones are equivalent in age is not necessarily true.
6. Shape of original cone—insufficient material may have been extruded to form a fully developed cone, and original shape is not determined by the angle of repose. Unless a cone has achieved full-stage growth, the ratios r/h and s/h and slope angles will indicate relative ages that are too old in comparison with fully developed cones.

These factors notwithstanding, field and photogeologic studies and the results of the present work suggest that many cones can be selected for which valid comparative age relationships can be established.

IMPLICATIONS FOR LUNAR STUDIES

As in many fields of young basaltic volcanic rocks, the features in the Lunar Crater volcanic field bear a strong resemblance to features on the moon. The vast majority of craters on the moon are like the aptly named Lunar Crater in that their floors are distinctly lower than their surroundings and their rims slightly higher. However, well-known impact craters such as Meteor Crater, Ariz., also have this gross morphology. Abundant criteria are present in the terrestrial craters to distinguish maars, of which Lunar Crater is a good example, from impact craters (Masursky, 1964). These include (1) lack of deformation of strata exposed in the walls of maars; (2) lack of a systematic sequence in materials composing the rims of maars other than grading or rude bedding produced by fallout and successive eruptions; and (3) presence on the rims of maars of new volcanic material often in the form of sideromelane or palagonite as well as preexisting rock from the exposed walls and the subsurface parts of the vent. Shock-induced structures and shock-phase mineralogy are absent in maars. In contrast, the strata exposed in the walls of impact craters are severely deformed (Milton, 1968) and, in the classic case of

Meteor Crater, are overturned (Shoemaker, 1962) so that they lie on the raised rim in reverse sequence from the normal stratigraphic succession in the walls. No new rock units not present in the eviscerated bowl are found in the ejecta on the rims; shock-induced structures and phases may be common.

Before manned exploration of the moon, craters were deduced to be either of impact or internal origin on the basis of areal distribution, structural alinement, crater shape, and the scale of explosive features. Some maarlike lunar craters form chains along pronounced structural trends; these occur along the Hyginus (fig. 9) and Abulfeda Rilles and in the Davy crater chain. Others, such as the dark-halo craters on the floor of Alphonsus (figs. 10, 11), are single craters on well-defined structural features. Apollo missions to one or more of these features are a possibility. Some of the features observed at Lunar Crater may be present at these locations, although the eroding effect of the impact of small particles may make it difficult to observe the structure in the walls or the nature and composition of the rim deposits. The presence of maars on the moon, if confirmed, would suggest that phreatic eruptions may have occurred there and that, in turn, permafrost may now be or once was present in the lunar subsurface (Fisher and Waters, 1969).

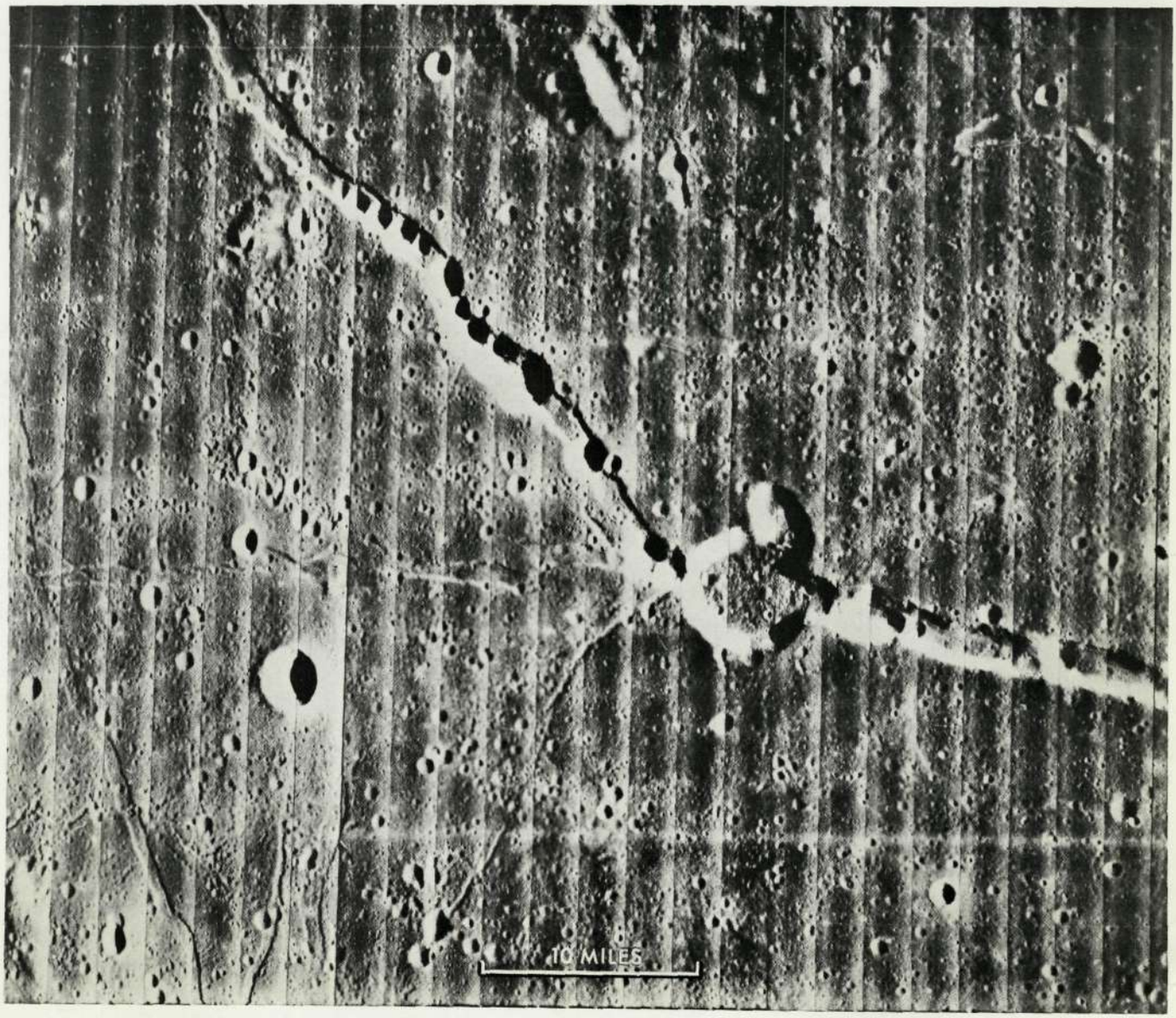

FIGURE 9.—The lunar crater Hyginus and the Hyginus Rille. Vertical and horizontal lines and streaks in this and other Lunar Orbiter photographs are artifacts of the photographic system. For additional views of this feature, see Cortright (1968, p. 104, 118). Lunar Orbiter V photograph.

FIGURE 10.—A dark-halo crater athwart a rille on the floor of the large lunar crater Alphonsus. Ranger IX photograph. (See also Cortright, 1968, p. 48.)

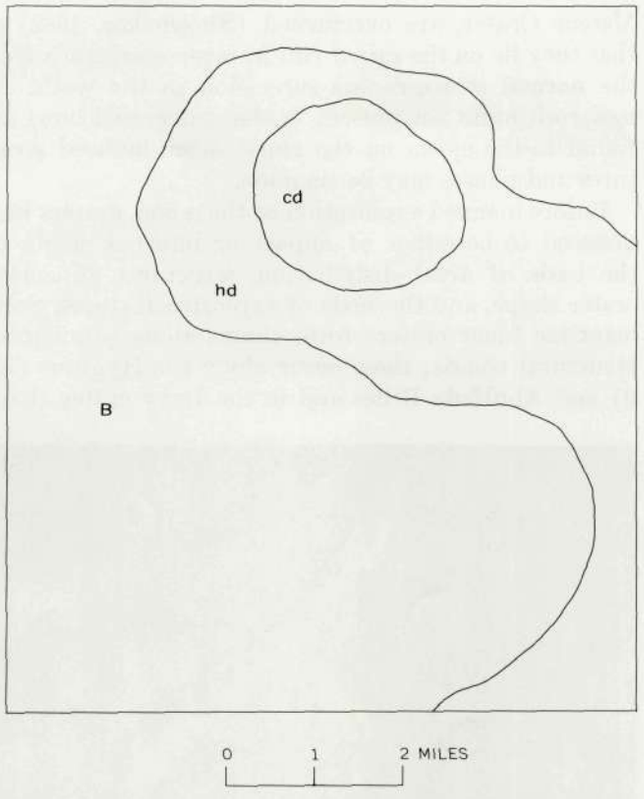

FIGURE 11.—Sketch map of the extent of a dark halo around a crater shown in figure 10. cd, material in and around dark-halo crater, fills adjacent rilles; hd, dark-halo material, no visible relief, seen best on photographs taken near full moon; B, basin-fill material, makes up largest part of the floor of the crater Alphonsus.

Although most craters on the moon have relatively low-lying floors like Lunar Crater or Meteor Crater, localized examples do occur of craters atop domes and of cones with floors higher than the ground beyond these protuberances. Foremost among these are the cratered hills of the Marius Hills region (fig. 12) (McCauley, 1969; Karlstrom and others, 1968). Domes with gentle slopes in this region are 150–300 feet high, and steep domes are 600–750 feet above the surrounding plains. The size and gross form of these features are similar to some of the cones in the Lunar Crater field (fig. 7), although in the lunar example, there are many small superposed craters on the domes and cones.

Particularly striking is the similarity between the linear pyroclastic vent north of Easy Chair Crater (fig. 3) and a prominent linear crater in the Marius Hills region (fig. 13). The lunar crater is alined along regional structural trends just as the crater in Nevada is alined parallel to the major line of craters in the field (fig. 6). An endogenetic origin of some form is certainly required for the linear crater on the moon. Another area of the moon where prominent linear craters appear to be structurally controlled is in the mare north of the crater Gruithuisen (fig. 14). Craters also occur at the summits of mounds and cones on the floor of Copernicus (Hartmann, 1968, p. 147) (fig. 15), in the highlands around Descartes west of the Nectaris basin (Wilhelms and McCauley, 1969) (fig. 16), and around the crater Zupus west of the Humorum basin (Wilhelms and McCauley, 1969) (fig. 17) where numerous linear craters are alined along regional tectonic directions.

Many lunar craters and other landforms have a highly subdued appearance with gentle slopes and no sharp features, in contrast to other craters and landforms which are sharp and fresh looking (fig. 18). Some form of erosion seems to have been operative on the lunar surface, although the rate of such erosion must be very low compared to terrestrial rates. Bombardment of the surface by very small particles from space has been suggested as the principal cause of this erosion (Ross, 1968; Soderblom, 1970). Erosion of craters by small particles on the moon may be nearly a constant volume process like the erosion described here

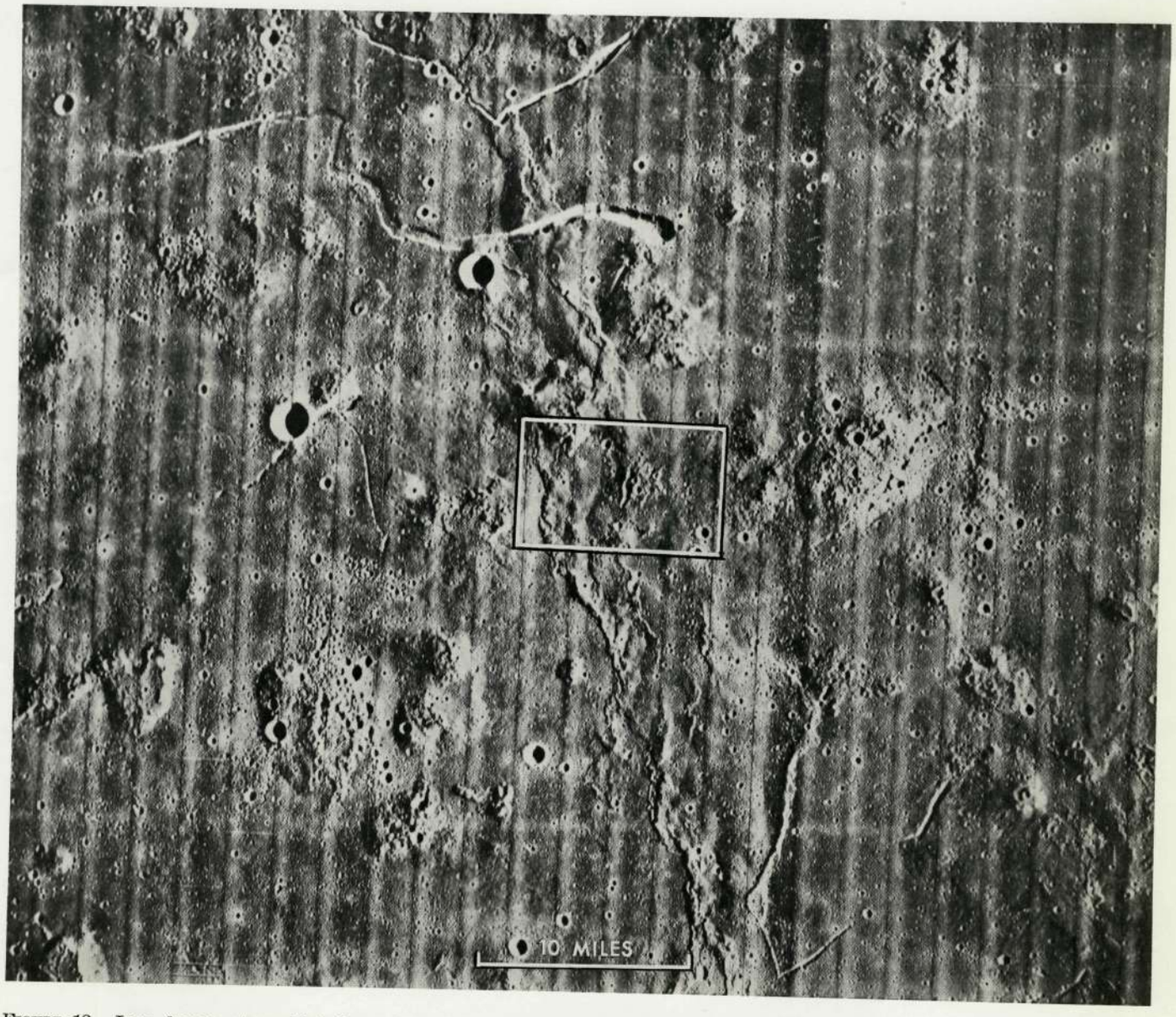

FIGURE 12.—Low domes, steep-sided domes, ridges, and rilles in the Marius Hills region of the moon. Outline shows area of figure 13. Lunar Orbiter V photograph. (See also Cartright, 1968, p. 90, 119.)

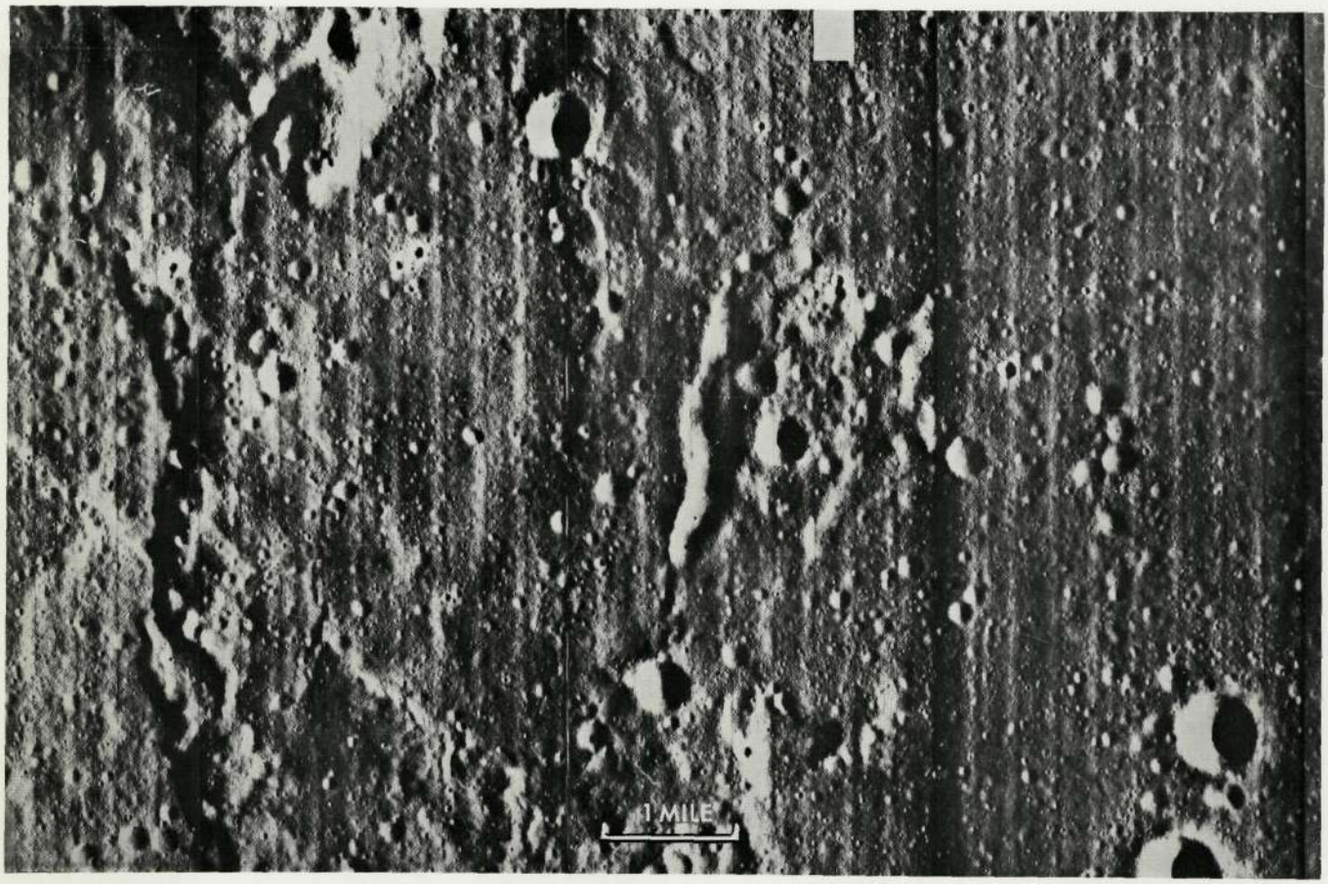

FIGURE 13.—A linear crater (center) approximately 1,500 feet wide in the Marius Hills region. Outline of area shown in figure 12. Lunar Orbiter V photograph.

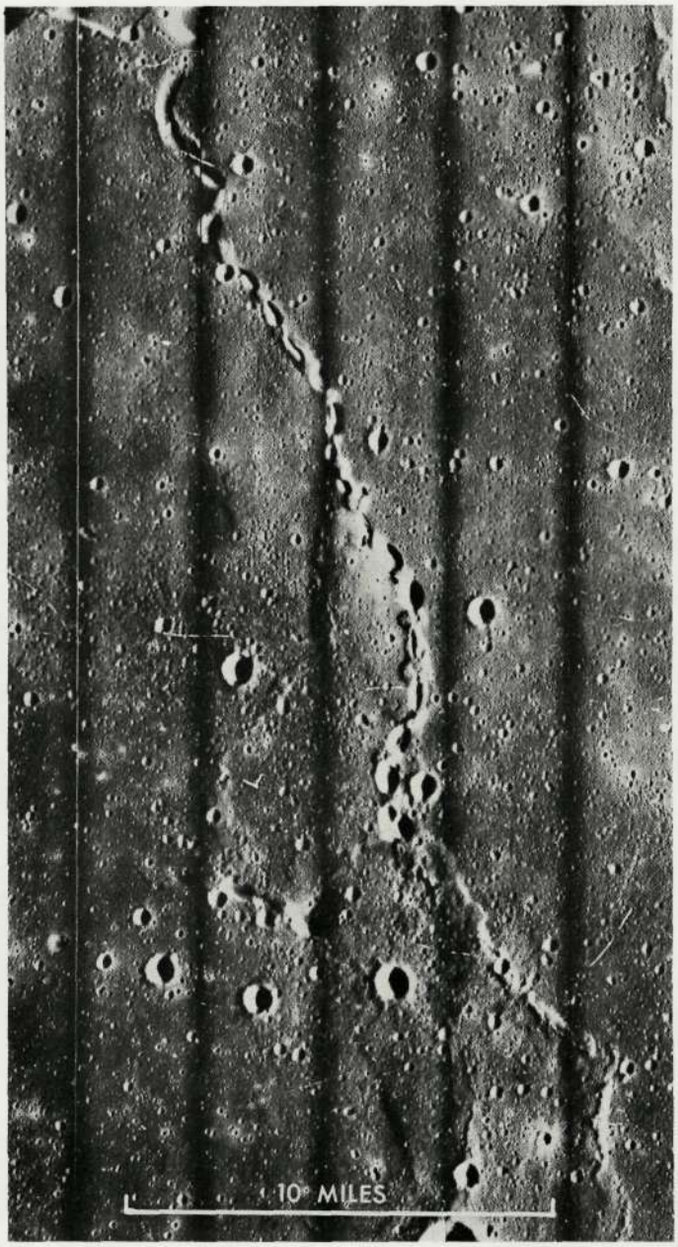

FIGURE 14.—A series of narrow linear craters on the mare material north of the crater Gruithuisen. The line of craters merges with a mare ridge at the bottom of the photograph. Lunar Orbiter V photograph.

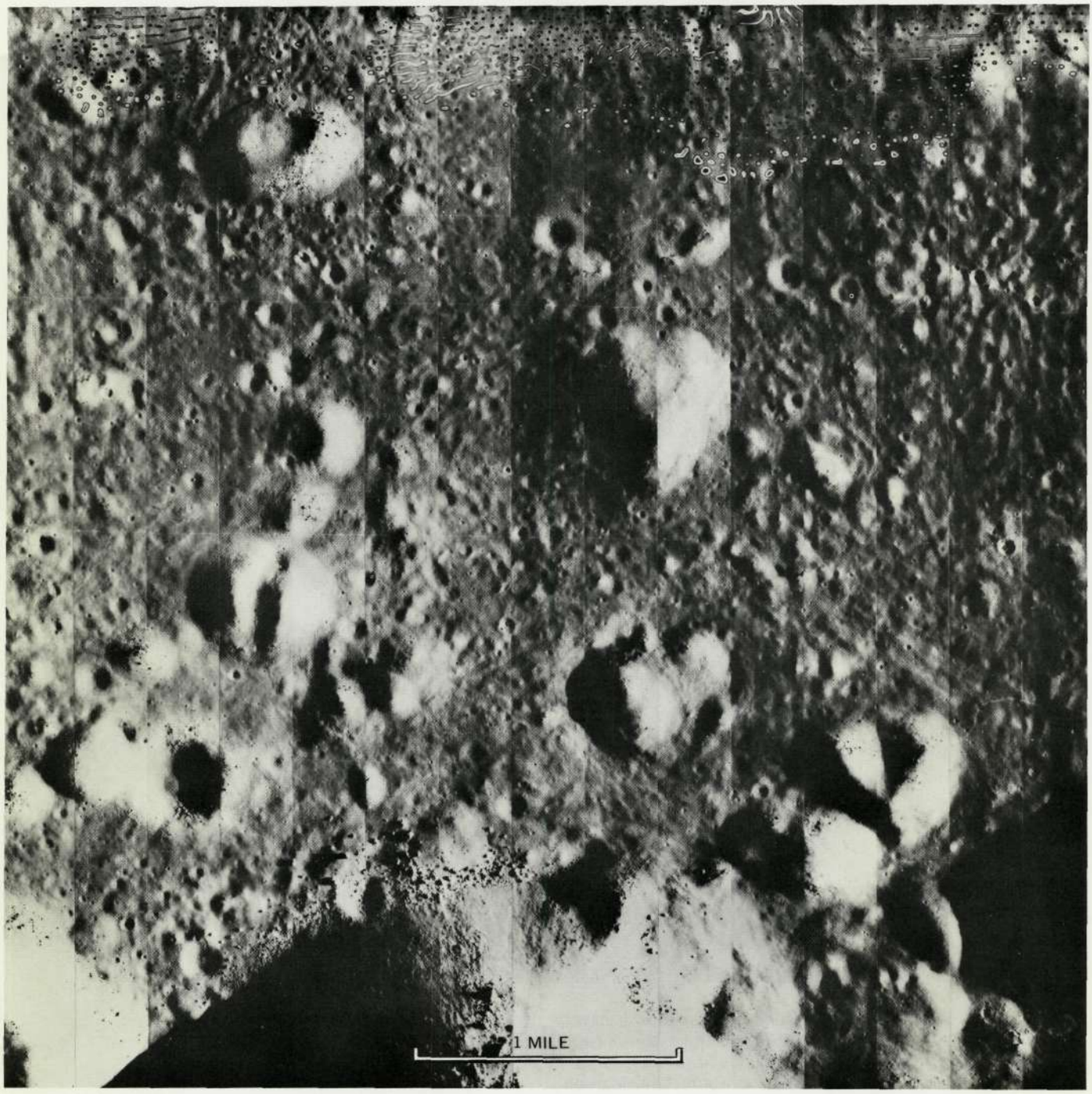

FIGURE 15.—Domes and hills with summit pits on the floor of the crater Copernicus. Large hill at the bottom of the photograph is part of the central peak of Copernicus. Lunar Orbiter V photograph.

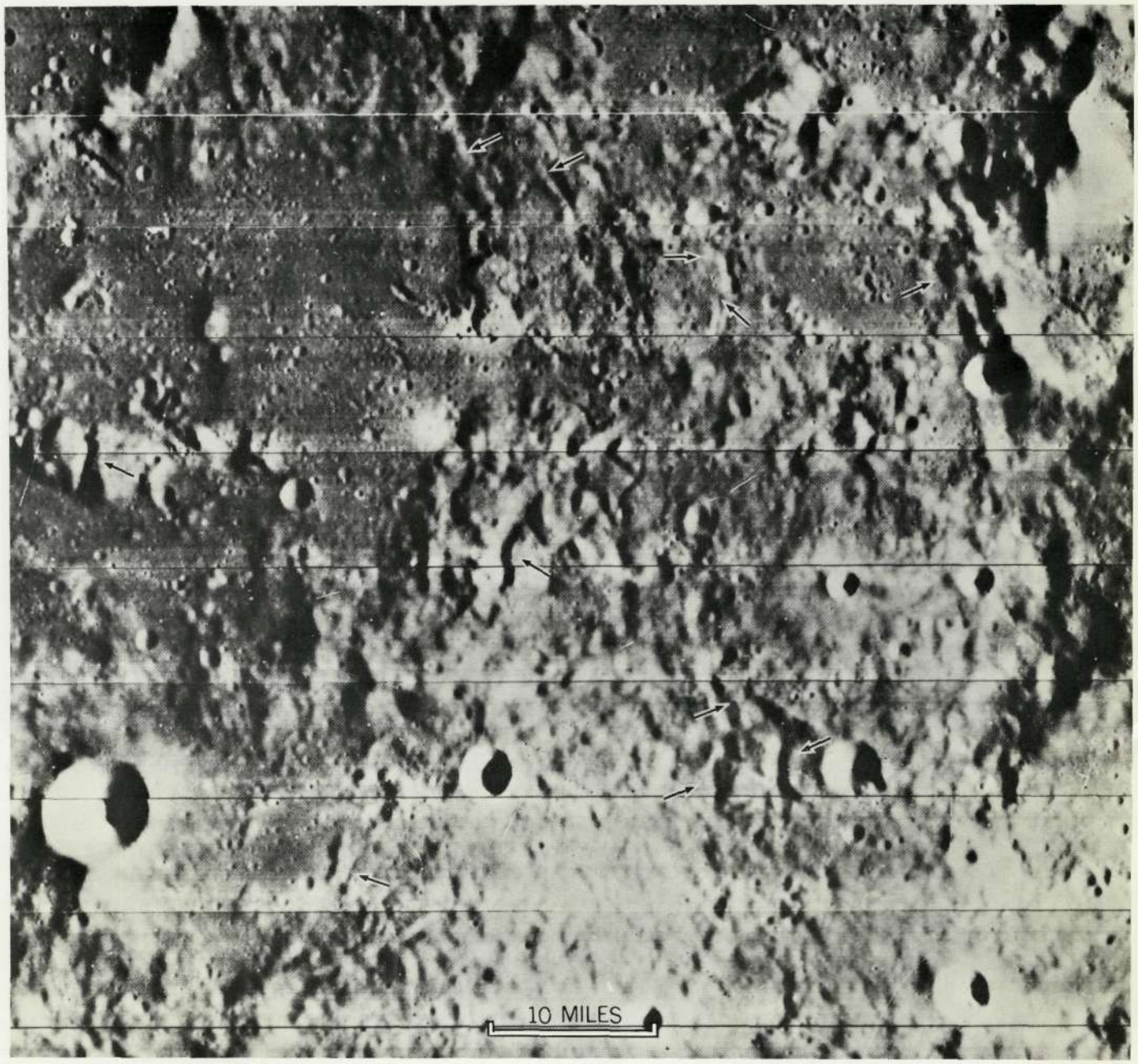

FIGURE 16.—The Descartes area in the lunar terrae with rough, hummocky, blanketing deposit studded with numerous steep domes and scattered irregular to linear craters (arrows). Lunar Orbiter IV photograph.

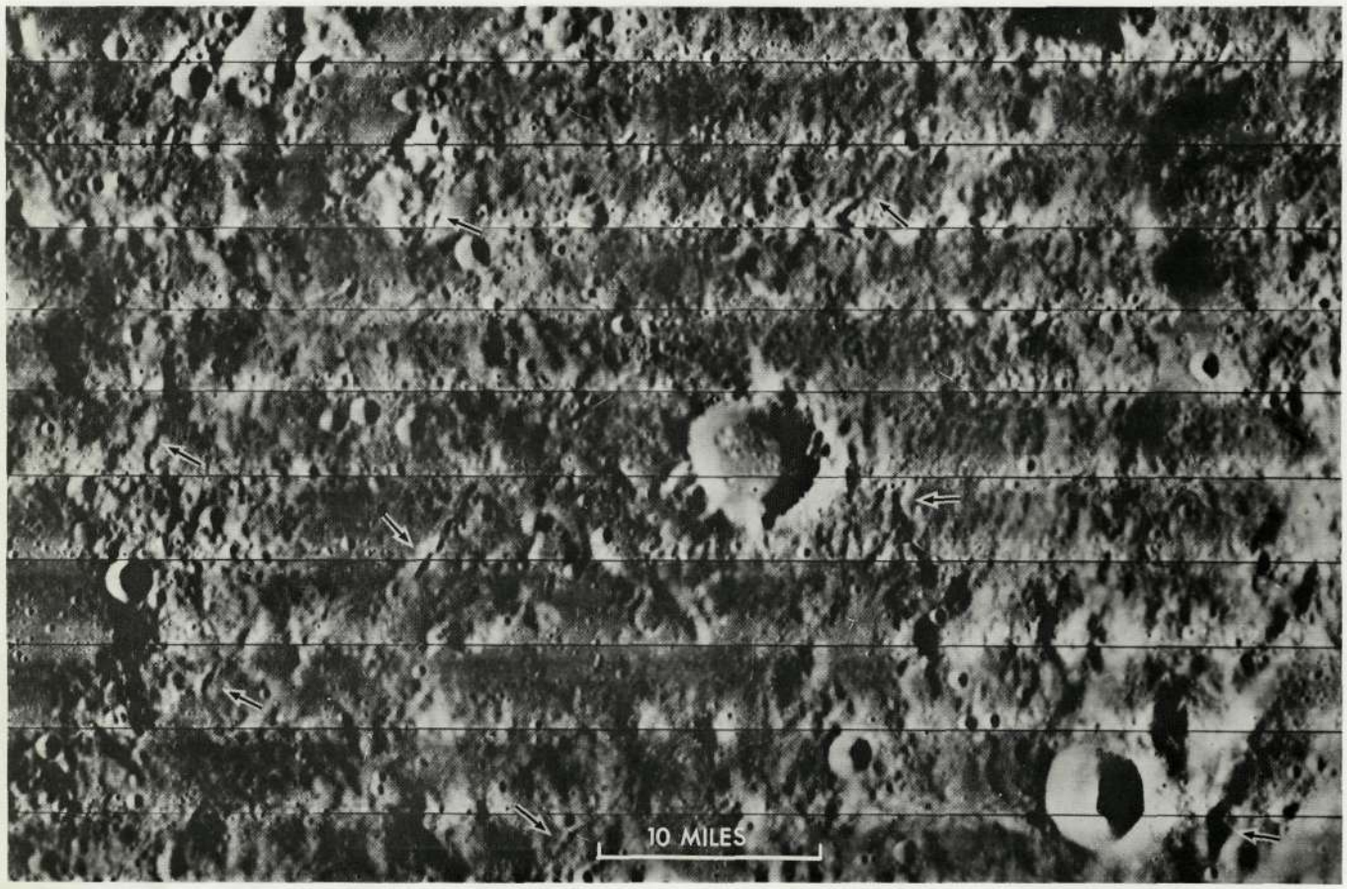

FIGURE 17.—Part of the lunar terrae west of Mare Humorum and south of the crater Zupus. Terrain similar to that shown in figure 13. Linear craters shown by arrows. Lunar Orbiter IV photograph.

in the Pancake Range of central Nevada. Although each impact of a small particle ejects a relatively large amount of material—between 10^2 and 10^3 of its own mass—some of it to relatively great distances, material is returned to any given site from distant impacts. Also, where slopes are steep enough, slumping and downslope rolling and sliding of particles will occur with every primary or secondary impact (Ross, 1968, p. 1345). Lunar craters should thus have a base to height ratio that increases with increasing age. Lunar Orbiter photographs appear to confirm this. However, precise measurements of crater heights and base widths, particularly of strongly subdued craters, have not yet been possible. Such measurements may be possible from better quality Apollo photography. Also exposure ages determined on samples from craters with a variety of ages may allow confirmation of age sequences deduced from photographic measurements and may give some indications of the rate of erosion.

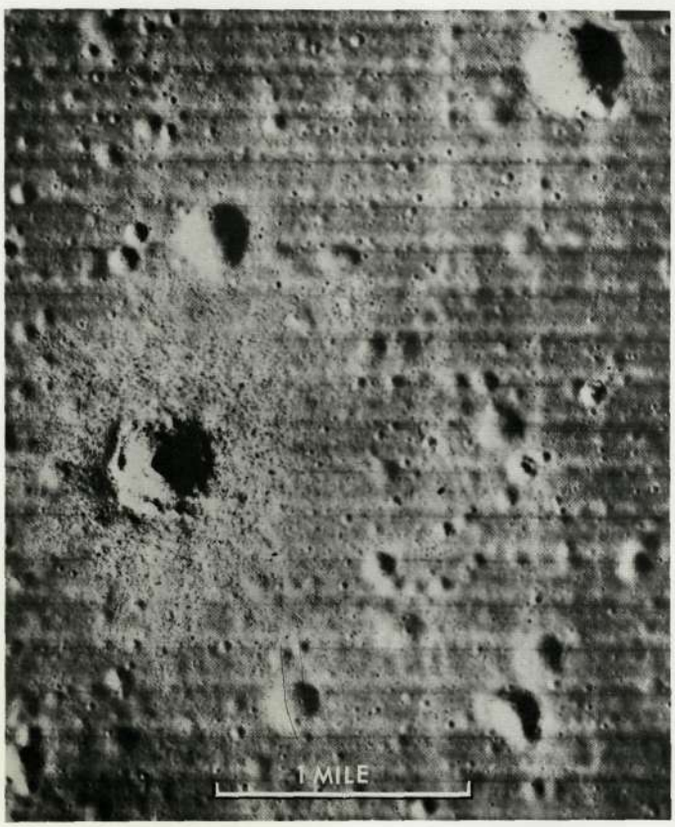

FIGURE 18.—Mare area in Oceanus Procellarum, showing gradation in crater morphology from sharp with strongly upturned rims to nearly rimless depressions. Most craters in this area were probably formed by impact. Lunar Orbiter III photograph.

REFERENCES

Armstrong, R. L., Ekren, E. B., McKee, E. H., and Noble, D.C., 1969, Space-time relations of Cenozoic silicic volcanism in the Great Basin of the western United States: Am. Jour. Science, v. 267, no. 4, p. 478–490.

Cook, E. F., 1965, Stratigraphy of Tertiary volcanic rocks in eastern Nevada: Nevada Bur. Mines Rept. 11, 61 p.

Cortright, E. M., ed., 1968, Exploring space with a camera: Nat. Aeronautics and Space Adm. Spec. Pub. 168, 214 p.

Fisher, R. V., and Waters, A. C., 1969, Bed forms in base-surge deposits—lunar implications: Science, v. 165, p. 1349–1352.

Green, D. H., and Ringwood, A. E., 1967, The genesis of basaltic magmas: Contr. Mineralogy and Petrology, v. 15, no. 2, p. 103–190.

Hartmann, W. K., 1968, Lunar crater counts VI—The young craters Tycho, Aristarchus and Copernicus: Arizona Univ. Lunar and Planetary Lab. Commun., v. 7, pt. 3, p. 145–156.

Karlstrom, T. N. V., McCauley, J. F., and Swann, G. A., 1968, Preliminary lunar exploration plan of the Marius Hills region of the Moon: U.S. Geol. Survey open-file report, 42 p.

Kleinhampl, F. S., and Ziony, J. I., 1967, Preliminary geologic map of northern Nye County, Nevada: U.S. Geological Survey open-file report, scale 1:200,000, 2 sheets.

MacDonald, G. A., 1969, Composition and origin of Hawaiian lavas, *in* Studies in vulcanology—A memoir in honor of Howel Williams: Geol. Soc. America Mem. 116, p. 477–522.

MacDonald, G. A., and Katsura, T., 1964, Chemical composition of Hawaiian lavas: Jour. Petrology, v. 5, no. 1, p. 82–133.

Masursky, Harold, 1964, A preliminary report on the role of isostatic rebound in the geologic development of the lunar crater Ptolemaeus, *in* Astrogeologic Studies Ann. Prog. Rept., July 1, 1963–July 1, 1964, pt. A: U.S. Geol. Survey open-file report, p. 102–134.

McCauley, J. F., 1969, The domes and cones in the Marius Hills regions—evidence for lunar differentiation? [abs.]: Am. Geophys. Union Trans., v. 50, no. 4, p. 229.

Milton, D. J., 1968, Structural geology of the Henbury meteorite craters, Northern Territory, Australia: U.S. Geol. Survey Prof. Paper 599–C, p. C1–C17.

Morrison, R. B., and Frye, J. C., 1965, Correlation of the middle and late Quaternary successions of the Lake Lahontan, Lake Bonneville, Rocky Mountain (Wasatch Range), southern Great Plains, and eastern Midwest areas: Nevada Bur. Mines Rept. 9, 45 p.

Rittman, A., 1962 Volcanoes and their activity: New York-London, Interscience Publishers, John Wiley & Sons, 305 p.

Ross, H. P., 1968, A simplified mathematical model for lunar crater erosion: Jour. Geophys. Research, v. 73, no. 4, p. 1343–1354.

Shoemaker, E. M., 1962, Interpretation of lunar craters, *in* Kopal, Zdeněk. ed., Physics and astronomy of the Moon: New York, Academic Press, p. 283–359.

Smith, A. L., and Carmichael, I. S. E., 1969, Quaternary trachybasalts from southeastern California: Am. Mineralogist, v. 54, nos. 5 and 6, p. 909–923.

Smith, R. L., 1960, Zones and zonal variations in welded ash flows: U.S. Geol. Survey Prof. Paper 354–F, p. 149–159.

Snyder, R. P., Ekren, E. B., and Dixon, G. L., 1969, Geologic map of Lunar Crater quadrangle, Nye County, Nevada: U.S. Geol. Survey open-file report.

Soderblom, L. A., 1970. A model for small-impact erosion applied to the lunar maria: Jour. Geophys. Research, v. 75, no. 14, p. 2655–2661.

Thorarinsson, Sigurdur, 1953, The crater groups in Iceland: Bull. Volcanol., ser. 2, v. 14, p. 3–44.

Trask, N. J., 1969, Ultramafic xenoliths in basalt, Nye County, Nevada, *in* Geological Survey research 1969: U.S. Geol. Survey Prof. Paper 650–D, p. D43–D48.

Vitaliano, C. J., and Harvey, R. D., 1965, Alkali basalt from Nye County, Nevada: Am. Mineralogist, v. 50, nos. 1–2, p. 73–84.

Wilhelms, D. E., and McCauley, J. F., 1969, Volcanic materials in the lunar terrae—Orbiter Observations [abs.]: Am. Geophys. Union Trans., v. 50, no. 4, p. 230.

Wise, W. S., 1969, Origin of basaltic magmas in the Mojave Desert area, California: Contr. Mineralogy and Petrology, v. 23, p. 53–64.

U.S. GOVERNMENT PRINTING OFFICE:1971 O—420-710

Page intentionally left blank